Thermodynamic and Kinetic Study on Phase Behavior of Binary Mixtures of POP and PPO Forming Molecular Compound Systems

A. Minato and S. Ueno

Faculty of Applied Biological Science, Hiroshima University, Higashi-Hiroshima 739, Japan

K. Smith

Colworth Laboratory, Unilever Research, Bedford, U.K.

Y. Amemiya

Faculty of Engineering, The University of Tokyo, Bunkyo-ku, Tokyo 113, Japan

K. Sato*

Faculty of Applied Biological Science, Hiroshima University, Higashi-Hiroshima 739, Japan

Received: September 25, 1996; In Final Form: February 28, 1997[⊗]

The phase behavior of PPO (*sn*-1,2-dipalmitoyl-*sn*-3-oleoylglycerol) and POP (sn-1,3-dipalmitoyl-*sn*-2-oleoylglycerol) binary mixture was examined using differential scanning calorimetry, conventional and synchrotron radiation X-ray diffraction (XRD), and highly pure samples. A molecular compound, β_C, was formed at the 1:1 concentration ratio of PPO and POP, giving rise to two monotectic phases of PPO/compound and compound/POP in a juxtapositional way. β_C has a long spacing value of 4.1 nm of double chain length structure. In the PPO/compound region, the DSC melting peak increased with increasing PPO concentration, whereas the DSC melting peak increased with increasing POP concentration in the compound/POP region. The melting point of β_C was lowest at 31.2 °C. Time-resolved XRD study unveiled the formation of molecular compounds in metastable forms, α_C and β'_C, having the same PPO/POP concentration ratio as β_C. α_C and β'_C exhibited monotectic phases with corresponding metastable forms of the pure components. In α_C, two hexagonal packing XRD short spacing peaks were obtained for α_C, corresponding to a differently packed hexagonal subcell of two leaflets. A structure model of the PPO/POP molecular compound is proposed, involving separation of palmitoyl chain leaflet and palmitoyl−oleoyl mixed-acid chain leaflet in the double chain length structure. This model justifies the structure of β_C of SOS/SSO proposed by Engstrom (Engstrom, L. *J. Fat Sci. Technol.* **1992** *94*, 173−181), in which the saturated and unsaturated chains are packed in the same leaflet of the double chain length. The present work additionally proved that the formation of the molecular compound was present in the α_C and β'_C metastable forms, as directly proved by dynamic X-ray diffraction study using synchrotron radiation.

Introduction

Triacylglycerols (TAGs) are major components of fats and oils that are abundantly present in biotissues. Together with proteins and carbohydrates, they are the most important nutrients. In industry, TAGs are used in oils, margarine, and confectionery fats etc., in foods, and as matrix materials in pharmaceuticals and cosmetics, etc.[1] In these real systems, the fat structures play dominant roles in determining physical properties such as texture, plasticity, and morphology.

Many fats present in the real systems are multicomponent in two ways: (a) a fat phase contains many different types of TAGs, and (b) each TAG molecule involves different types of fatty acid moieties, namely mixed-acid TAGs. Therefore, physical analysis of the multicomponent systems must deal with an understanding of pure materials and, at the same time, with an elucidation of mixed systems.[2−6] The best approach for the latter task is to study binary systems in terms of their major TAGs. The detailed study of the binary mixture may reveal the nature of molecular interactions between the component materials. Three typical phases occur in binary solid mixtures, when the two components are miscible in all proportions in a liquid state: solid solution phase, eutectic phase, and compound formation. The general tendency in the relationship between the molecular interactions and the phase behavior may be summarized as follows; structural affinity results in solid solutions, poor interactions form eutectic phases, and specific interactions give rise to molecular compounds.

For the mixtures of acylglycerols, phase behavior is rather complicated for two reasons: polymorphism and acyl chain compositions attached to the glycerol group. For example, in the mixture of monosaturated acid TAGs, a eutectic phase with a limited region of solid solution is formed for the stable form when the chain length difference is no larger than two carbon atoms. However, metastable forms of α and β' exhibit solid solution phases.[7] Similar results were reported for the mixtures of optically active diacylglycerols.[8] As for the acyl chain composition, no solubility of the monosaturated acid TAG was obtained in a crystal of *cis*-monounsaturated acid TAG.[7] An interesting study, however, recently showed that the effect of the *trans*-configuration of the double bond is to modify the phase behavior through partial solubilization in the mixtures EEE−OOO and EEE−SSS (E, elaidoyl).[9] As for the formation of the compound systems, the occurrence of compound formation

* Corresponding author: Tel, +81-824-24-7935; Fax, +81-824-22-7062.
[⊗] Abstract published in *Advance ACS Abstracts,* April 1, 1997.

S1089-5647(96)02956-2 CCC: $14.00

in particular sets of TAG mixtures were suggested in such mixtures as SOS/SSO (1,2-distearoyl-3-oleoylglycerol) and POP/OPO (P = palmitoyl).[2,7] Moran indicated two binary systems, in juxtaposition, of POP/compound and compound/OPO, in which the compound was estimated to form at an equal concentration ratio, but the details were missing.[10] Most recently, Engstrom[11] and Koyano et al.[12] reported precise analyses of the mixture systems of SOS/SSO and SOS/OSO, respectively, both claiming a compound was formed at a concentration ratio around 1:1.

The formation of a molecular compound observed in SOS/SSO and SOS/OSO indicates specific molecular interactions through the acyl chain moieties. It is worthy to note that oleoyl chains are present in both components of the above two mixture systems of saturated-oleic mixed-acid TAGs.[11,12] The structure model proposed for the SOS/OSO compound assumed segregation of stearic and oleic acid chains to form a double chain length structure.[12] This is in contrast to the triple chain length structure of each component TAG, SOS, and OSO.[13,14] These results indicate that olefinic interaction may play a key factor in the formation of a molecular compound. In this regard, FT-IR[15] and solid-state NMR[16] analyses showed that the oleoyl chain exhibits quite complicated conformational structures during polymorphic transformation of SOS and POP. As for the SOS/SSO mixture, the metastable form of α exhibited a solid solution, yet the molecular compound system was revealed in the most stable forms. Therefore, it is interesting to elucidate the molecular structures and kinetic properties of the mixture systems forming the molecular compounds. However, little work has been reported on this subject. The use of a time-resolved synchrotron radiation X-ray beam may facilitate this task; yet, the work so far available has been concerned with PPP/SSS[17−19] and POP/PPP[20], and neither are miscible nor compound forming in the stable forms.

The present work deals with the phase behavior of the molecular compound forming systems of binary mixtures of PPO (*rac*-1,2-palmitoyl-3-oleoyl triacylglycerol) and POP (*sn*-1,3-palmitoyl-2-oleoyl triacylglycerol) using different scanning calorimetry (DSC) and X-ray diffraction with conventional and synchrotron radiation. The polymorphic behavior of POP and PPO are described in an order of thermodynamic stability in the following: PPO, α (3) and β'(3),[21] and POP, α-2, γ-3, β'-2, β_2-3, and β_1-3, where 2 and 3 refer to double and triple chain length structure. Although two additional metastable forms have been reported for POP,[13] conversion in the chain length structure from double−triple−double−triple is curious behavior, which does not occur in PPO. As for the mixture system of PPO and POP, contradiction is still evident in literature; eutectic phase behavior was suggested by Moran,[10] yet compound formation was indicated by Rossell.[22] It should be stressed that the mixture of PPO and POP is of practical importance, since palm oil, a promising fat resource, involves high concentrations of POP and PPO which jointly determine the physical properties of palm oil-blended fats.

Materials and Methods

POP and PPO were provided by Unilever Research Laboratory (Colworth, U.K.) with purity higher than 99%. The binary mixtures of PPO and POP were prepared by mixing the weighed samples at room temperature, melting them above 50 °C, rapidly cooling to 0−10 °C, and tempering at different temperatures. The melting points of the most stable forms of POP and PPO are 36 °C (β_1) and 35 °C (β'), respectively. The most stable forms were formed by incubating the mixtures at 29 °C over 90 days.

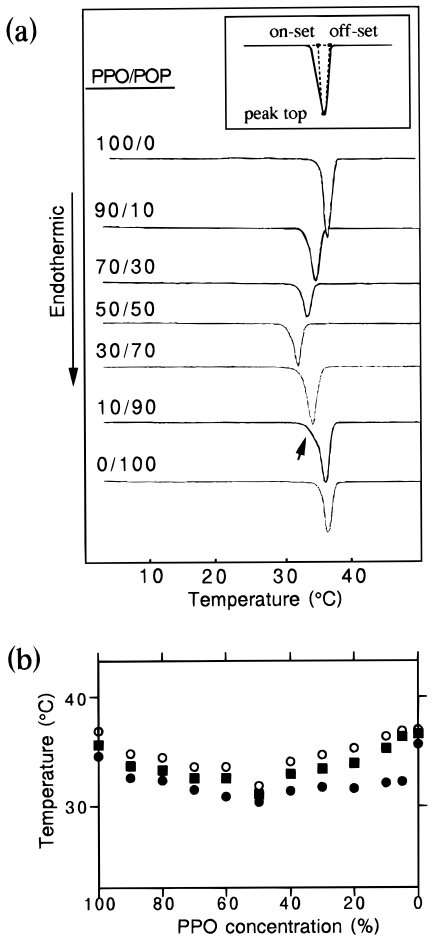

Figure 1. (a) DSC heating thermogram of the most stable forms of PPO/POP mixtures. (b) Onset (●), peak-top (■), and offset (○) temperatures.

The transformation and melting behavior of the mixtures were measured by DSC (Rigaku DSC-8230) at a rate of 2 °C/min. The crystal forms were measured by powder X-ray diffraction (XRD) (Rigaku Geigerflex and Rotaflex RU-200, λ = 0.1542 nm for both). Synchrotron radiation X-ray diffraction (SR-XRD, λ = 0.15 nm) was taken at the Photon Factory (PF) in the National Laboratory for High-Energy Physics, Tsukuba, Japan. PF operates at 2.5 GeV. The X-ray diffraction spectra were recorded every 10 s with two gas-filled one-dimensional position sensitive detectors. One is for the small-angle region (Rigaku, Tokyo, 512 channels over a total length of 200 mm), the other is for the wide-angle region (MAC Science, Tokyo, 512 channels over a total length of 50 mm), and the distance between sample and the detector was 1280 mm (small-angle) and 280 mm (wide angle). The temperature of the sample was controlled by two water baths and recorded in combination with X-ray diffraction data collection.

Results

Figure 1a shows DSC heating thermograms of the most stable forms of the mixtures at various concentration ratios of PPO/POP obtained by incubating at 29 °C over 90 days. The peaks of pure PPO around 35.6 °C and POP around 36.2 °C correspond to the melting of β' and β_1, respectively. With increasing concentration of POP, endothermic peaks decreased to 31.2 °C at the POP 50% concentration. Above the POP 50% concentration, endothermic peaks shifted to higher temperature ranges until the melting point of β1 of POP was reached. It is notable that a shoulder peak appeared below the main melting

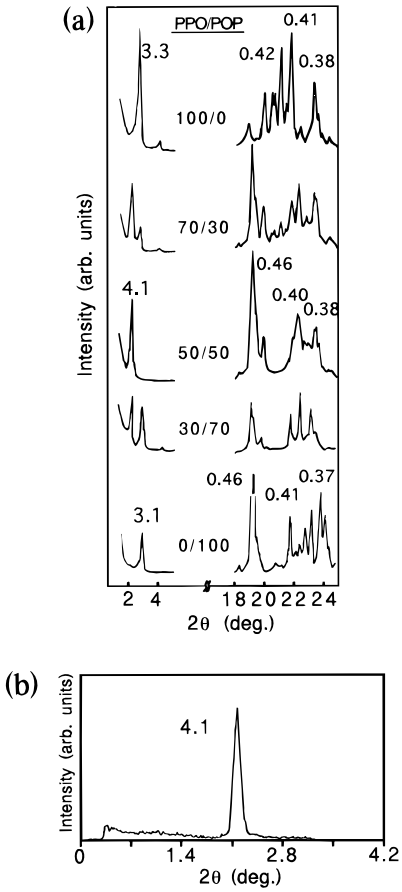

Figure 2. Wide-angle and low-angle X-ray diffraction spectra of the most stable forms of (a) PPO/POP mixtures taken at 20 °C, (b) a small angle X-ray diffraction spectrum of β_C of PPO/POP = 50/50 mixture taken at 20 °C (unit, nm).

peak at POP 90%, as shown by an arrow. This peak was also observed in the mixture of PPO/POP = 5/95. It was found that the most stable form of this peak corresponds to the melting of the compound (see below).

Figure 1b shows three temperatures as defined to represent the melting in Figure 1a: onset, peak-top, and offset as defined in Figure 1a. It is notable that offset and peak-top temperature showed minima at the POP 50%, yet the onset temperature revealed a plateau at the POP concentration of 10%−95%. No increase in the melting temperature at the POP 50% was detectable in any types of peak temperature.

The conventional XRD spectra are shown in Figure 2a. The low-angle peaks of 3.3 nm (PPO) and 3.1 nm (POP) correspond to the (002) reflection of long spacings of 6.6 nm and 6.2 nm in the triple chain length structure. The mixtures of PPO/POP of 70/30 and 30/70 exhibited additional peaks at 4.1 nm. The 50/50 mixture only showed the 4.1 nm peak as shown in the small-angle XRD spectra (Figure 2b). This peak is the (001) reflection of the molecular compound containing a 1:1 ratio of PPO and POP with a double chain length structure. The separation of the two peaks of 4.1 and 3.3 nm at the 70/30 mixture and 4.1 and 3.1 nm at the 30/70 mixture is proof that the molecular compound is immiscible with POP and PPO. As an evidence of this, it is notable that the intensity of 4.1 nm was higher than those of other peaks in the two mixtures. This can be explained by considering the concentration ratios of the compound and pure materials. For example, in PPO/POP = 70/30 the compound consists of 60% (compound: PPO 30% + POP 30%) and 40% of PPO. A similar interpretation can be applied to the POP 70% mixture.

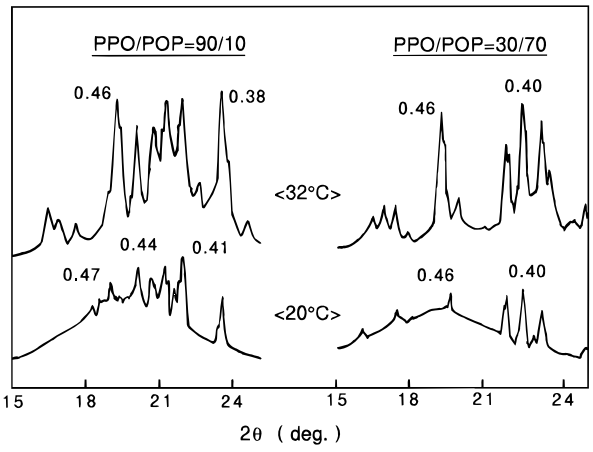

Figure 3. Temperature dependence of XRD short spacing spectra of the most stable forms of PPO/POP mixtures (unit, nm).

As for the wide-angle reflection of Figure 2a, pure PPO and POP exhibited the typical short spacing patterns of β' and β_1, respectively.[13,22] The short spacing patterns of the molecular compound (50%) resemble those of the molecular compounds of SOS/OSO and SOS/SSO, categorized as β having triclinic subcell structure.[11,12] Herewith, the β form of the molecular compound will be called β_C. The short spacing patterns of the 70/30 and 30/70 mixtures are the superposition of those of PPO β' and β_C, and POP β_2 and β_C, respectively. The different occurrence of β_2 and β_1 of POP in Figure 2a will be discussed later.

Figure 3 shows the temperature dependence of XRD short spacing spectra of the most stable forms of the PPO/POP mixtures of 90/10 and 30/70. The XRD pattern at 20 °C of each mixture equals that of the 70/30 and 30/70 mixtures, respectively. However, the XRD patterns of β_C disappeared by raising the temperature to 32 °C where PPO β' and POP β_2 appeared together with liquid lines. The same data were obtained in other concentration ratios. This clearly shows the monotectic nature of the mixture of β'_{PPO}/β_C and β_C/β_{POP}.

From here, experimental data of metastable forms obtained by DSC and SR-XRD will be shown in a combined manner. Figure 4a shows DSC heating thermogram of the PPO/POP = 90/10 mixture, which was quenched from 50 °C and incubated for 15 min at 0 °C and then subjected to heating DSC analysis at a rate of 2 °C/min. Because of the complexity of the thermogram, we will refer here to the peak-top melting pint. A small endothermic peak appeared at 10.2 °C, and a large endothermic peak appeared at 18.3 °C, which was followed by an exothermic peak around 20 °C. There was a shoulder peak at 15.7 °C, as shown by an arrow. Further heating exhibited a broad exothermic peak around 26 °C and a large endothermic peak at 29.3 °C. Except for the peak at 10 °C, the total behavior quite resembles a typical pattern of α melting followed by the crystallization of the next stable form which then melts, as observed in SSS (α melt, β crystallization, and β melt).[4] However, the SR-XRD data have shown that the polymorphic occurrences and transformations of the molecular compound and PPO are simultaneously involved in the DSC data of Figure 4a.

Figure 4b shows low- and wide-angle SR-XRD spectra, taken under the temperature variation profile shown in an inserted figure. Soon after 10 °C was reached, a small peak appeared in low-angle region, having long spacing of 4.9 nm. Upon incubation at 10 °C, the peak of 4.9 nm continuously shifted to 4.6 nm, and a new spectrum of 3.9 nm appeared 50 s after the occurrence of the 4.9 nm peak. Correspondingly, a short

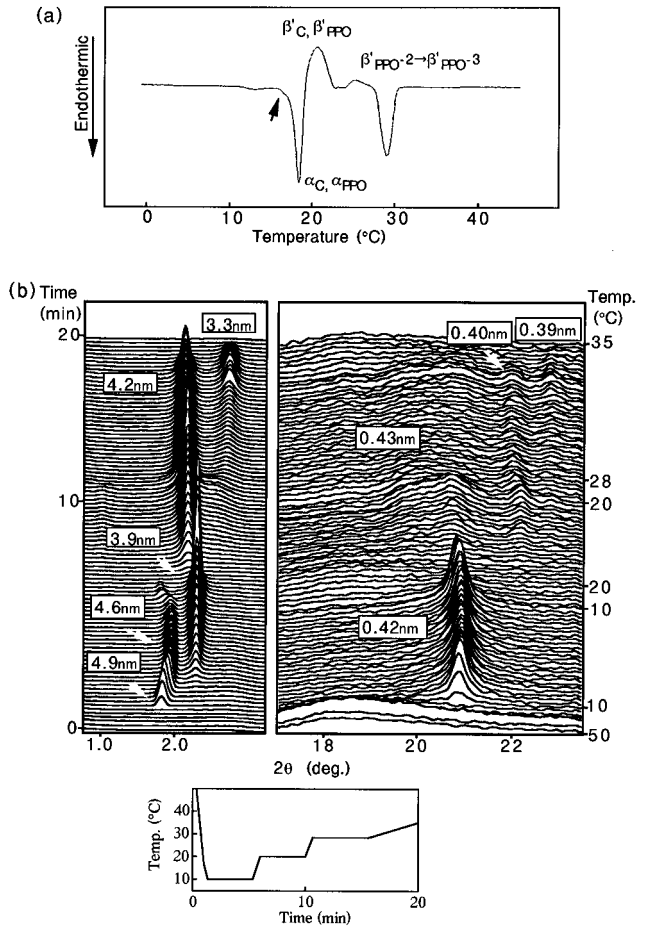

Figure 4. (a) DSC heating thermogram and (b) synchrotron radiation X-ray diffraction spectra of metastable forms of PPO/POP = 90/10 mixture.

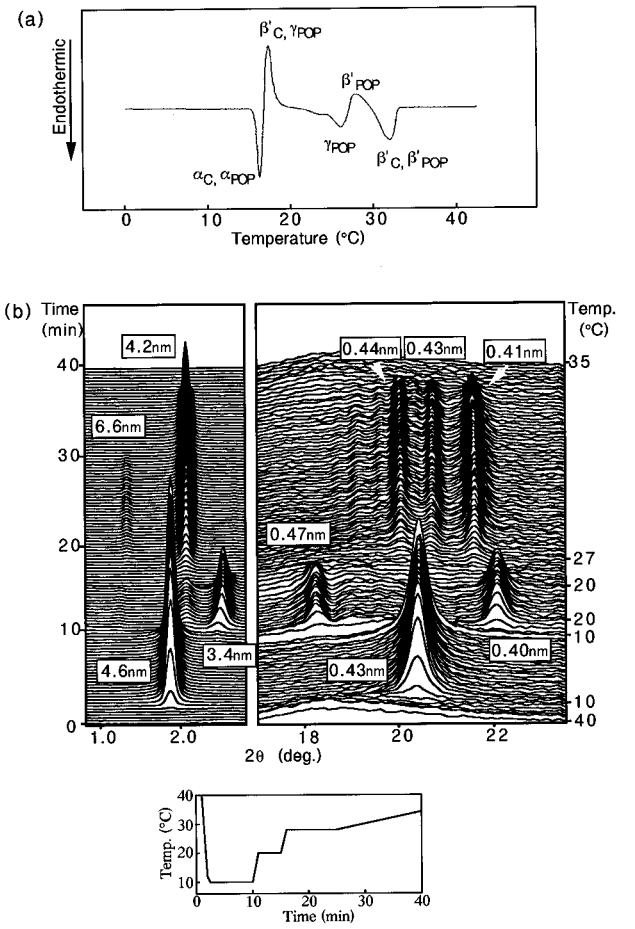

Figure 5. (a) DSC heating thermogram and (b) synchrotron radiation X-ray diffraction spectra of metastable forms of PPO/POP = 5/95 mixture.

spacing spectrum of 0.42 nm appeared at 10 °C in the wide-angle region. Since the α form of PPO has a long spacing value of 7.8 nm with a triple chain length structure,[21] the spectrum of 3.9 nm in Figure 4b corresponds to the (002) reflection of α_{PPO}. Thus, the spectrum of 4.9 and 4.6 nm is due to the α form of a molecular compound with double chain length structure (α_C). Hence, two α forms occurred at 10 °C. The temperature jump from 10 to 20 °C induced the melting of the two α forms, as shown in the low- and wide-angle diffractions of Figure 4b. It is notable that long spacing peak at 4.6 nm of α_C slightly moved to 4.9 nm, which soon disappeared before the disappearance α_{PPO}. Hence, the DSC endothermic peaks at 18.3 °C in Figure 4a correspond to the two α forms. However, no corresponding data are detectable in SR-XRD for the small endothermic peak at 10.2 °C. This may be due to the occurrence of less stable forms, although not resolved in the present work.

Soon after the melting of α, new forms having a sharp long spacing spectrum of 4.2 nm and a broad spectrum around 3.5 nm appeared, both corresponding to the exothermic peak around 20 °C in Figure 4a. The temperature jump from 20 to 28 °C induced the conversion from broad to sharp peaks at 3.3 nm, yet the peak at 4.2 nm was almost unchanged. Correspondingly, three short spacing spectra of 0.42, 0.40, and 0.39 nm gradually appeared and increased in their intensity in the wide-angle region, although their intensity was low. These spectra are characteristic of β'. Since β'_{PPO} has a long spacing value of 6.6 nm with triple chain length,[21] the spectrum of 3.3 nm is the (002) reflection of β'_{PPO}. Thus, the spectrum of 4.2 nm is due to β' of the molecular compound (β'_C). A separation of β'_{PPO} and β'_C indicates the monotectic nature of the system. Upon heating, the two β' forms disappeared at around 32 °C in Figure 4b, which is higher than the melting point at 28.6 °C shown in Figure 4a. This discrepancy may be ascribed to difference in thermal treatment; the SR-XRD experiment underwent incubation at 20 °C, which may increase the melting point of β' forms of two crystals. The broad exothermic peak around 25 °C corresponds to changes in chain length structure of β'_{PPO} from double (001 reflection, 4.2 nm) to triple (002 reflection, 3.3 nm), as revealed in Figure 4b after the temperature jump from 20 to 28 °C. It follows that the concentration ratio of α_C/α_{PPO} and β'_C/β'_{PPO} in the PPO/POP = 90/10 mixture is 20/80, which agrees with the intensity ratio of the long spacing peaks of the two α forms. However, the intensity of the long spacing of β'_{PPO} is abnormally low compared to β'_C. This was confirmed by the influence of chain length conversion from double to triple in β'_{PPO}, although not shown here. After long incubation at 28 °C, the long spacing spectrum of the triple chain length of β'_{PPO} became stronger than β'_C and β_C.

Figure 5 shows DSC and SR-XRD data of the metastable forms of the PPO/POP = 5/95 mixture. In this concentration ratio, the separation of the XRD spectra of the compound (10% concentration) and POP (90% concentration) was most clearly revealed. The heating thermogram, in Figure 5a, showed a large endothermic peak at 15.0 °C, which was soon followed by an exothermic peak at around 18 °C. These two peaks correspond to the melting of the less stable forms and rapid crystallization of the more stable forms. Further heating showed two melting peaks at 26.5 and 32.0 °C, between which an exothermic peak at around 28 °C was seen. The SR-XRD showed that the DSC data in Figure 5a involved melting of α, crystallization and melting of β'_C, and β'_{POP} to which the occurrence of γ was added. The low- and wide-angle SR-XRD peaks of 4.6 and

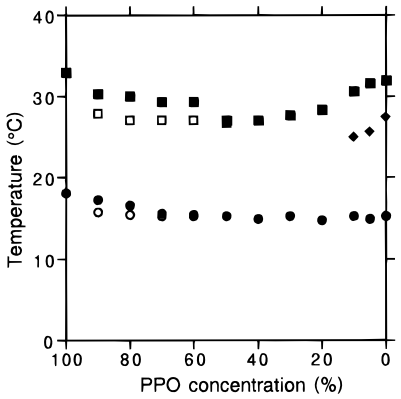

Figure 6. DSC melting points of metastable forms of PPO/POP mixtures.

0.43 nm at 10 °C correspond to α_C and α_{POP}, which exhibit the same XRD pattern. The temperature jump to 20 °C induced the melting of the two α forms, as shown in the disappearance of the peaks in the SR-XRD. At 20 °C, two long spacing peaks appeared, 4.2 nm of β'_C of double chain length (001) reflection and 3.4 nm of γ_{POP} of triple chain length (002) reflection. The intensity ratio of the two peaks agrees with the concentration ratio of compound and POP. The corresponding short spacing of 0.47 and 0.40 nm are characteristic of γ.[13] Hence, the monotectic nature of β'_C and γ_{POP} is revealed. A further temperature jump induced the melting of γ_{POP} at 25.6 °C, followed by the crystallization of β' of POP. Although not shown here, the heating DSC pattern of the 50/50 mixture showed two melting peaks at 15.5 and 26.8 °C, corresponding the melting of α_C and β'_C, respectively. Therefore, the disappearance of the low-angle SR-XRD of β'_C in Figure 5b is due to the solubilization of β'_C caused by the increase of the liquid POP fraction by the melting of γ_{POP}. The short spacing spectra of 0.44, 0.43, and 0.42 nm are typical of the β' of POP,[13] and the long spacing peak of 4.2 nm is the (001) reflection of β'_{POP} of double chain length structure. Weak long spacing peaks at 6.7 and 3.35 nm are due to the δ form POP of triple chain length structure,[13] which occurred concurrently with double chain length β' as a transient stable form. The melting of β'_{POP} is shown in the SR-XRD around 33 °C, slightly higher than the melting point exhibited by DSC.

Figure 6 summarizes the DSC endothermic peak-top temperature of melting of metastable forms occurring in the PPO and POP mixtures. The data of the 50/50 mixture correspond to the melting of pure α_C and β'_C. Additional peaks in the concentration ratios close to POP are due to γ_{POP} fractions.

Discussion

Phase Behavior. The present experiments using SR-XRD have shown that a molecular compound was formed at the 1:1 concentration ratio of PPO and POP, exhibiting α, β', and β forms. The occurrence of α and β' metastable forms was revealed by the use of SR-XRD. Figure 7 shows a phase diagram of the most stable form (a) and metastable forms (b) (a kinetic phase diagram).

As for the stable forms, Figure 7a shows monotectic phases formed between β_C and β_{POP}, where two β forms of POP are not differentiated. β_C is singly formed at the concentration ratio of PPO:POP = 1:1. In the PPO concentration above 50%, β'_{PPO} and β_C are formed below the melting point of β_C of 31 °C, and above that temperature β'_{PPO} and mixture liquid are present. This was clearly observed by XRD as shown in Figure 2a. However, no clear distinction of the melting peaks of β_C and β'_{PPO} was detectable by DSC heating (Figure 1a). This is caused

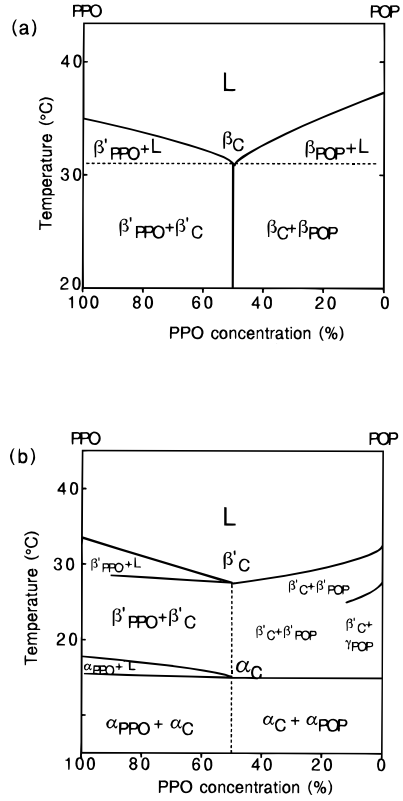

Figure 7. Phase diagrams of (a) stable forms and (b) metastable forms of PPO/POP mixtures.

by overlapping of the two endothermic peaks. Similarly, β_C and β_{POP} coexisted in the PPO concentration regions below 50% and below 29 °C. Thermal and structural data of β_C, β'_{PPO}, and β_{POP} are summarized in Table 1, together with those of α_C and β'_C polymorphs of POP and PPO, and two other mixture systems of SSO/SOS and SOS/OSO.

This phase behavior in Figure 7a may be rather curious in such a sense that there is no increase in the melting point of β_C without showing eutectic behavior between the compound and each pure component, as often observed in the compound formation mixtures, and also shown in SOS/SSO.[11] However, the behavior of Figure 7 can be explained by solubility of β'_{PPO} and β_{POP} in mixture liquid, using the following equation[23]

$$\ln x_B = -\Delta H_f/R(1/T - 1/T_m)$$

where x_B is the molar solubility of a solid equilibrated with mixture liquid, ΔH_f is the enthalpy of fusion, T_m is the melting point, and R is the gas constant. Although this equation applies to ideal solution, one may calculate the temperature of β'_{PPO} and β_{POP} equilibrated with mixture liquid at $x_B = 0.5$, using the experimental data of ΔH_f and T_m in Table 1. The calculated results are 29 °C (β'_{PPO}), 32 °C ($\beta_{1\ POP}$), and 30 °C ($\beta_{2\ POP}$). These values are almost the same as or even higher than T_m of β_C, 31 °C. Therefore, it is not possible to exhibit eutectic behavior in the combination of $\beta'_{PPO}-\beta_C$ and $\beta_C-\beta_{POP}$.

The presence of metastable α_C and β'_C forms were confirmed in the molecular compound of PPO/POP as shown in Figure 7b. The basic behavior of monotectic nature is the same as that for β forms, namely, α_C and β'_C are not miscible with corresponding forms of PPO and POP. The monotectic behavior was most evidenced by different long spacing values of α_{PPO} and α_C as clearly shown by SR-XRD (Figure 4b). The immiscible property between α_C and α_{POP} and β'_C and β'_{POP} was not verified by DSC and SR-XRD, since their melting and structure properties are quite similar. However, the presence

TABLE 1: Thermal and Structural Properties of Polymorphic Forms of PPO/POP Compound, PPO, POP, SSO/SOS Compound, and SOS/OSO Compound[a]

	PPO/POP (1:1)[b]			PPO[c,d]		POP[e]				
	α_c	β'_c	β_c	α	β'	α	γ	β'	β_2	β_1
T_m (°C)	15.5	28.0	31.2	18.5	35.2	15.2	27.0	33.5	35.1	36.7
ΔH_f	na	90	97	na	104	na	92.5	98.3	124.4	130.2
ΔS_f	na	0.30	0.32	na	0.34	na	0.31	0.32	0.40	0.42
LS (nm)	4.6	4.2	4.1	7.8	6.5	4.65	6.54	4.24	6.10	6.10
SS (nm)	0.43	0.43	0.46	0.415	0.46	0.425	0.47	0.44	0.46	0.46
	0.42	0.39	0.40		0.44		0.39	0.42	0.41	0.38
			0.38		0.42			0.41	0.39	0.37
					0.40			0.40	0.38	
					0.38				0.37	
									0.36	

	SSO/SOS[f]		SOS/OSO[g]
	α_c	β_c	β_c
T_m (°C)	26	40.6	36
ΔH_f	na	124	135.3
ΔS_f	na	0.39	0.44
LS (nm)	8.3	4.5	4.5
SS (nm)	0.4	0.46	0.46
		0.39	0.36
		0.37	0.38

[a] T_m, melting point; ΔH_f, enthalpy of fusion (kJ/mol); ΔS_f, entropy of fusion ((kJ/mol)/deg); LS, long spacing; SS, short spacing; na, not available. [b] Present work. [c] Reference 21. [d] Reference 11. [e] Reference 13. [f] Reference 11. [g] Reference 12.

of the γ form at POP concentrations above 90% is the proof of immiscibility as shown in Figure 5b. To compare the results in Figure 7 with SSO/SOS and SOS/OSO, two major differences must be discussed: α was miscible in SSO/SOS, and no β'_C was observed in SSO/SOS and SOS/OSO. As for the presence of α in SOS/OSO, it was observed in limited concentration ranges, yet it transformed quite rapidly to more stable forms. The authors assume that the above two differences may be ascribed to differences in thermal treatment of the samples and time resolution of the XRD measurement. In the present DSC measurement examining the metastable forms, the molten sample was quenched and, soon after, heated to prevent the transformation to more stable forms. Time-resolution by SR-XRD was 10 s, which is short enough to follow the crystallization and melting of metastable forms. Therefore, re-examination of SSO/SOS and SOS/OSO using SR-XRD may enrich the understanding of the phase behavior of the two mixture systems. Finally, it is worthwhile to compare the present result with the kinetic phase behavior of PPP/POP examined by SR-XRD.[20] All of the stable β and unstable α and β' forms in the PPP/POP mixtures are immiscible, yet no compound formation was observed.

Structures of Molecular Compound. The structures of TAG crystals are characterized by chain length structure, subcell structure, and methyl end packing.[3,6] In order to discuss the structure models of the three forms of α_C, β'_C, and β_C of the molecular compound of 1:1 combination of PPO and POP, long and short spacing XRD spectra and DSC entropy of fusion are available, as discussed for the compound of SOS/OSO.[12]

The long spacing values of the three forms showed double chain length structure as illustrated in Figure 8. Unlike the SOS/OSO mixture, the numbers of oleoyl and palmitoyl chains are not balanced. Hence, the oleoyl and palmitoyl chains must be packed together in either leaflet in the double chain length lamellae like model A or in both leaflets (model B). This may cause intensity in molecular conformation and, thereby, the subcell structure compared to the β_C of SOS/OSO.[12] However, the XRD short spacing spectra have shown that α_C and β'_C and β_C revealed the typical patterns of the subcell structure of H (hexagonal), $O_\perp$ (orthorhombic perpendicular), and $T_{||}$ (triclinic parallel), respectively. Each pattern is typical of monosaturated acid TAGs. This might seem curious, since it is expected that some deviation would be caused by steric hindrance between the oleoyl and palmitoyl chains which is the driving force for the chain sorting to form the triple chain structures in the stable forms of SOS and POP.[13,15] In this regard, an intensity feature was observed in precise XRD measurements as splitting of short spacing spectra of α.

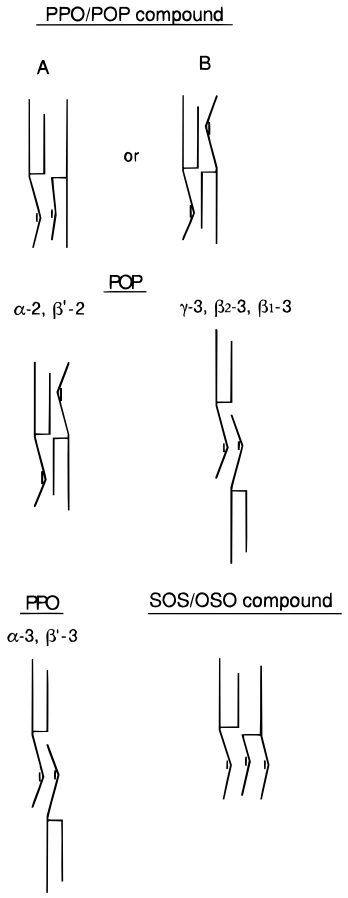

Figure 8. Structure models of PPO/POP compound, PPO, and POP.

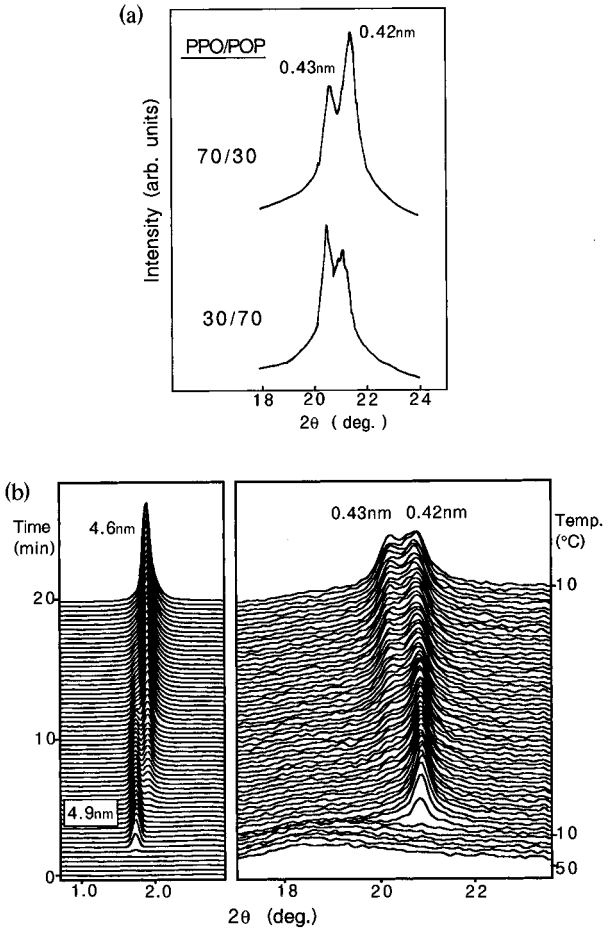

Figure 9. (a) Conventional and (b) synchrotron radiation X-ray diffraction spectra of PPO/POP mixtures.

Figure 9a shows the splitting of short spacing spectra of α_C. The splittings in 0.43 and 0.42 nm were clearly detectable. This splitting was observed in a range of the PPO concentrations from 80% to 20%. The intensity ratio of two peaks was reversed between the 70/30 and 30/70 mixtures, and equal intensity was seen in the 50/50 mixtures. As a dynamic process, Figure 9b shows SR-XRD spectra of the 50/50 mixture taken by quenching to 10 °C and incubating at that temperature over 60 min. The first occurring α_C had long spacing of 4.9 nm and single short spacing of 0.42 nm. Sixty seconds after this occurrence, both the low- and wide-angle spectra started to change as follows: long spacing was shortened to 4.6 nm, and a new short spacing spectrum appeared at the same time as the shifting of long spacing. The stabilized short spacing spectra consisted of 0.42 and 0.43 nm with the same intensity. This behavior can be interpreted by considering the influence of steric hindrance between the oleoyl and palmitoyl chains in α_C for the structure model of A (Figure 8).

To begin with, it is necessary to note that the short spacing value of triple chain length α of PPO, 0.415 nm, is shorter than double chain length α of POP, 0.425 nm (Table 1). This is due to the absence of repulsive interaction between the oleoyl and palmitoyl chains in α_{PPO} since the two chains are separated. However, the steric hindrance caused the extension or expansion of H packing in α_{POP} of double chain length. As for α_C, the stabilized subcell packing may be different in the two leaflets. If one takes the model A of α_C, one leaflet only contains palmitoyl chains while palmitoyl and oleoyl chains coexist in the other leaflet. Therefore, the short spacing value must be smaller in the former leaflet, compared to the latter leaflet. This is the same as that which was observed in Figure 9b. The first occurring α may contain fluid-like acyl chains having larger long spacing and shorter small spacing values compared to the stabilized α. Then the stabilization may induce the repulsive steric hindrance between the oleoyl and palmitoyl chains, causing the subcell packing of the lower leaflet of model A to become extended. As a result, two short spacings are formed. It follows that the PPO 70% mixture containing 60% α_C and 40% α_{PPO} must have the stronger spectrum of 0.42 nm because of the enriched contribution by more compact hexagonal packing. By contrast, the PPO 30% mixture must have the weaker spectrum of 0.42 nm, as shown in Figure 9a. This interpretation cannot be made, if model B is taken for the PPO/POP compound. Consequently, the basic structure model of A is most plausible for α_C. This model justifies the structure of β_C of SOS/SSO proposed by Engstrom,[11] in which the saturated and unsaturated chains are packed in the same leaflet of the double chain length. The present work additionally proved that the formation of the molecular compound was present in the α_C and β'_C metastable forms, as directly proved by dynamic X-ray diffraction study using synchrotron radiation.

The detailed molecular structures of β'_C and β_C, and even of α_C, are open to future work, although model A in Figure 8 is most plausible. The elucidation must be down on structures of mixed-acid leaflet in terms of precise subcell packing and conformation, glycerol structures, and methyl end packing. In this regard, it is worth stressing that *cis*-unsaturated fatty acids can exhibit quite diverse molecular structures, as observed in oleic acid,[6,25,26] erucic acid,[26,27] petroselinic acid,[28] and asclepic acid.[29] This diversity may be seen in the subcell structures of the saturated-oleoyl mixed-acid TAGs in pure components[15,30,31] and their mixtures.[11,12] For this purpose, the use of multitechniques such as FT-IR will be quite useful, and work along these lines is in progress.

The ordering state in the crystal phase can be discussed on the basis of the entropy of fusion, ΔS, which is 0.32 (J/mol)/deg for β_C of PPO/POP. This value is smaller than those of OSO (β, $\Delta S = 0.46$ (J/mol)/deg), POP β_1 (0.42 (J/mol)/deg), and SOS/OSO (0.44 (J/mol)/deg). However, the value is comparable to PPO β' 0.34 (J/mol)/deg, and SSO/SOS β_C is intermediate. Entropy of fusion indicates the difference of ordering between crystal and melt, so the β_C of PPO/POP is more liquid-like than the compound of SOS/OSO and SSO/SOS. We assume that this would be attributed to the difficulty in arranging compact packing of oleoyl chains in the same leaflet in β_C, because of its bent geometrical structure of oleoyl chains.

As a final argument, practical application will be discussed. Granular crystal formation in fats containing palm oil in such products as margarine and shortening is the cause of sandy taste and loss of gloss in the end products. The XRD analyses have shown that the granular crystals are of β type having triple chain length structures.[32−34] From the present study, the possibility of this being the β_C of PPO/POP is excluded, since it has double chain length structure. In addition, the transformation from β_2 to β_1 in POP was remarkably retarded in the POP fraction present in the PPO/POP mixture, as shown in Figure 2. This may be the result of the influence of the presence of PPO or PPO/POP compound on the polymorphic transformation of POP. This result might suggest a means for developing an antibloom effect for cocoa butter fat, which involves a high concentration of POP.

Acknowledgment. The authors are deeply indebted to Dr. H. Seto for providing us a data analysis software for SR-XRD measurements.

References and Notes

(1) Formo, M. W. In *Bailey's Industrial Oil and Fat Products*; Swern, D., Ed.; John Wiley & Sons: New York, 1979; Vol. 1, pp 177−232.

(2) Timms, R. E. *Prog. Lipid Res.* **1984**, *23*, 1−38.

(3) Small, D. M. *The Physical Chemistry of Lipids*; Plenum: New York, 1986; Chapter 10, pp 345−395.

(4) Hagemann, J. W. In *Crystallization and Polymorphism of Fats and Fatty Acids*; Garti, N., Sato, K., Eds.; Marcel Dekker: New York, 1988; pp 9−95.

(5) deMan, J. M. In *Fatty Acids in Food and Their Health Implications*; Chow, C. K., Ed.; Marcel Dekker: New York, 1992; pp 17−45.

(6) Sato, K. In *Advances in Applied Lipid Researches*; Padley, F., Ed.; JAI Press: New York, 1996; Vol. 2, pp 213−268.

(7) Rossell, J. B. *Adv. Lipid Res.* **1967**, *5*, 353−408.

(8) Iwahashi, M.; Ashizawa, K.; Kaneko, Y.; Muramatsu, M. *Bull. Chem. Soc. Jpn.* **1984**, *57*, 956−959.

(9) Desmedt, A.; Culot, C.; Deroanne, C.; Durant, F.; Gibon, V. *J. Am. Oil Chem. Soc.* **1990**, *67*, 653−660.

(10) Moran, D. P. *J. Appl. Chem.* **1963**, *13*, 91−100.

(11) Engstrom, L. *J. Fat Sci. Technol.* **1992**, *94*, 173−181.

(12) Koyano, T.; Hachiya, I.; Sato, K. *J. Phys. Chem.* **1992**, *96*, 10514−10520.

(13) Sato, K.; Arishima, T.; Wang, Z. H.; Ojima, K.; Sagi, N.; Mori, H. *J. Am. Oil Chem. Soc.* **1989**, *66*, 664−674.

(14) Kodali, D. R.; Atkinson, D.; Redgrave, T. G.; Small, D. M. *J. Lipid Res.* **1987**, *28*, 403−413.

(15) Yano, J.; Ueno, S.; Sato, K.; Arishima, T.; Sagi, N.; Kaneko, F.; Kobayashi, M. *J. Phys. Chem.* **1993**, *97*, 12967−12973.

(16) Arishima, T.; Sugimoto, K.; Kiwata, R.; Mori, H.; Sato, K. *J. Am. Oil Chem. Soc.* **1996**, *73*, 1231−1236.

(17) Kellens, M.; Meeussen, W.; Riekel, C.; Reynaers, H. *Chem. Phys. Lipids* **1990**, *52*, 79−98.

(18) Kellens, M.; Meeussen, W.; Gehrke, R. *Chem. Phys. Lipids* **1991**, *58*, 131−144.

(19) Kellens, M.; Meeussen, W.; Hammersley, A.; Reynaers, H. *Chem. Phys. Lipids* **1991**, *58*, 145−158.

(20) Minato, A.; Ueno, S.; Yano, J.; Wang, Z. H.; Seto, H.; Amemiya, Y.; Sato, K. *J. Am. Oil Chem. Soc.* **1996**, *73*, 1567−1572.

(21) Lutton, E. S. *J. Am. Chem. Soc.* **1951**, *73*, 5595−5598.

(22) Rossell, J. B. *Chem. Ind.* **1973**, 832−835.

(23) Hildebrand, J. H.; Scott, R. L. In *Solubility of Nonelectrolytes*; Reinhold: New York, 1950; pp 270−299.

(24) Suzuki, M.; Ogaki, T.; Sato, K. *J. Am. Oil Chem. Soc.* **1985**, *62*, 1600−1604.

(25) Kobayashi, M.; Kaneko, F.; Sato, K.; Suzuki, M. *J. Phys. Chem.* **1986**, *90*, 6371−6378.

(26) Kaneko, F.; Yamazaki, K.; Kobayashi, M.; Sato, K.; Suzuki, M. *Spectrochim. Acta* **1994**, *50A*, 1589−1603.

(27) Sato, K.; Yoshimoto, N.; Suzuki, M.; Kobayashi, M.; Kaneko, F. *J. Phys. Chem.* **1990**, *94*, 3180−3185.

(28) Yoshimoto, N.; Suzuki, M.; Sato, K. *Chem. Phys. Lipids* **1991**, *57*, 67−73.

(29) Larsson, K. *Fette Seifen. Anstrichm.* **1972**, *76*, 136−142.

(30) Hernqvist, L.; Larsson, K. *Fette Seifen Anstrichm.* **1982**, *84*, 349−354.

(31) Kawamura, K. *J. Am. Oil Chem. Soc.* **1979**, *56*, 753−758.

(32) Kawamura, K. *J. Am. Oil Chem. Soc.* **1980**, *57*, 48−52.

(33) Watanabe, A.; Tashima, I.; Matsuzaki, N.; Kurashige, J.; Sato, K. *J. Am. Oil Chem. Soc.* **1992**, *69*, 1077−1080.